processes

MDPI

Article

Production of Biochar via Pyrolysis of Apricot Seed Pulp with Calcium and Sodium Lignosulfonate

Ayşe Nihan Açıkkapı [1], Yahia Bani Hani [2], Hamiyet Şahin Kol [2] and Mehmet Kuddusi Akalın [2,*]

[1] Department of Chemistry, Karabük University, 78050 Karabük, Turkey; aysenihanacikkapi@karabuk.edu.tr
[2] Department of Environmental Engineering, Karabük University, 78050 Karabük, Turkey; yaheabanihani@gmail.com (Y.B.H.); hsahinkol@karabuk.edu.tr (H.Ş.K.)
* Correspondence: mehmetakalin@karabuk.edu.tr

Abstract

In recent years, due to increasing concerns about the environment and sustainable production, the effective utilization of wastes has become important. In this regard, it has become essential to obtain products with distinct properties by utilizing different types of biomass together. The world's annual apricot production is approximately 4 million tonnes. The apricot seeds can be used to produce seed oils; however, remaining residue (apricot seed pulp) from this process is considered as waste. In this study, the co-pyrolysis of waste from the essential oil industry (apricot seed pulp, ASP, and by-products of the paper pulp industry (calcium lignosulfonate, CLS, and sodium lignosulfonate, SLS)) was carried out using mixtures at different temperatures (400–700 °C) and different ratios (4:1, 1:1, 1:4). The effects of temperature and ratio on the yields, composition, and HHV of biochars were investigated. Among biochars obtained from co-pyrolysis, the maximum HHVs of 26.91 MJ·kg^{-1} and 25.64 MJ·kg^{-1} were obtained for 5ASP-5CLS-400 biochar and 8ASP-2SLS-400 biochar, respectively. The results showed that the addition of ASP to CLS led to an increase in the HHVs of biochars when compared to the HHVs of biochars obtained from the pyrolysis of CLS. The use of two different types of waste has led to the production of biochars with different properties due to the synergistic effect in the pyrolysis. As a result, biochars with diverse properties, which have the potential to be utilized in various applications, were produced from different types of wastes.

Keywords: apricot seed pulp; calcium lignosulfonate; sodium lignosulfonate; pyrolysis; biochar; waste valorization

check for updates

Academic Editor: Francesca Raganati

Received: 5 November 2025
Revised: 3 December 2025
Accepted: 8 December 2025
Published: 15 December 2025

Citation: Açıkkapı, A.N.; Bani Hani, Y.; Şahin Kol, H.; Akalın, M.K. Production of Biochar via Pyrolysis of Apricot Seed Pulp with Calcium and Sodium Lignosulfonate. *Processes* **2025**, *13*, 4053. https://doi.org/10.3390/pr13124053

Copyright: © 2025 by the authors. Licensee MDPI, Basel, Switzerland. This article is an open access article distributed under the terms and conditions of the Creative Commons Attribution (CC BY) license (https://creativecommons.org/licenses/by/4.0/).

1. Introduction

Biomass is a promising renewable resource for producing a wide variety of products for different purposes. Biomass is a renewable and abundant resource that can be regarded as a sustainable solution in the production of environmentally friendly products. A wide variety of biomass resources, such as corn residue [1], rice husks [2], and hazelnut shells [3], have been converted into value-added products through various conversion technologies. In addition to being a renewable resource, what distinguishes biomass is that it can be used as a carbon source, unlike other renewable resources such as solar and wind energy. Carbon-based materials produced from biomass have many potential uses, including as biofuels, in electrochemical processes, for adsorption, and in soil applications.

Pyrolysis is an inexpensive thermochemical method that has been utilized for many years to decompose materials in an oxygen-free environment and is also employed commercially. The pyrolysis process of biomass can yield a wide range of products, each

with distinct properties, including biofuel, fine chemicals, and carbon-based materials. In addition to the type of raw material used, pyrolysis parameters such as temperature, heating rate, and pyrolysis time are important in obtaining different types of products and product characteristics [4]. Furthermore, the co-pyrolysis process, which treats two or more diverse raw materials in the same pyrolysis system, is a widely employed technique to obtain products with varied characteristics [5]. The interaction between the decomposition mechanisms of these materials during the pyrolysis process enables the exploitation of the structural properties of both materials. Moreover, this process enables the concurrent evaluation of two waste raw materials, thus contributing to sustainable production by facilitating their conversion into high-value-added products. For instance, it is feasible to achieve higher-quality bio-oil through the co-pyrolysis of biomass and plastics [6]. Alternatively, carbon-based materials with improved properties can be obtained with the use of different types of wastes (i.e., municipal solid waste, plastic waste) in the pyrolysis process. Therefore, their effectiveness in supercapacitor and adsorption applications can be enhanced [4,5].

Apricot is classified under the rosaceae family, and it is used to make juices and canned products. Global apricot production is approximately 4 million tons, with Turkey accounting for about 22% of this total [7]. The seeds, which are a by-product of the apricot fruit, constitute roughly 7% of the fruit [8], and they can be used in the production of oil and cosmetics.

The apricot seed pulp (ASP) generated as a byproduct of apricot seed oil production contains amygdalin, a naturally occurring cyanogenic glycoside in the seed, which poses toxicological limitations for both human and animal consumption [8]. Therefore, the utilization of ASP for energy production and the generation of value-added products through safe and sustainable technologies is of great importance. In a previous study, defatted apricot seeds using n-hexane were pyrolyzed under CO_2 and N_2 atmosphere using a quartz tubular reactor. The biochars obtained from the pyrolysis of defatted apricot seeds were used in the transesterification of apricot oil in the study [9]. There are also studies in which apricot stones [10,11], apricot pulp [12], and apricot kernel shells [13] were used in pyrolysis to obtain products for various applications.

Lignocellulosic biomass, one of the most common biomass sources on a global scale, consists primarily of cellulose, hemicellulose, and lignin. Lignin is a renewable aromatic natural polymer, which is the second most abundant land-based bioresource after cellulose. It is also a by-product resulting from the utilization of cellulose and hemicellulose [14,15]. Its abundant availability and high oxygen content make it available for use as a natural adsorbent and precursor of activated carbon [16]. Lignosulfonate (LS), a by-product of the paper and pulp industry, is a water-soluble natural polymer with an aromatic and complex three-dimensional network structure. LS can be considered as a sustainable precursor of carbon and sulfur sources due to the sulphonate groups it has. Due to their unique properties, LSs can be used as, but are not limited to, animal feed, surfactants, lubricants, and stabilizers [16–20]. LSs constitute 90% of the total market share for commercial lignin. Their production is extensive on a global scale, with an estimated annual output of approximately 1 million tons of dry matter [20,21]. CLS and SLS are among the various types of lignin which are produced from the paper and pulp industry [22]. CLS is a highly promising material due to several factors. It is biodegradable, non-toxic, and eco-friendly. Furthermore, it is inexpensive and contains reactively functional groups [17]. SLS, which is a product from the sulfite pulping of lignin, contains many oxygen-containing functional groups. The interaction of numerous β-O-4′ and α-O-4′ linkages in lignin with sulfonic acid groups results in an improvement in its water solubility [23].

In recent years, LSs have been used to prepare carbon-based materials for various applications. NiS/activated carbon composites were produced for supercapacitor application using SLS as a precursor [24]. Carbon spheres as activated carbon precursors were produced by the hydrothermal carbonization of SLS at 230 °C for 16 h. In another study, it was used as a raw material to prepare a high-efficiency catalyst for the synthesis of dimethyl adipate [25]. SLS was also used with biochar derived from pretreated waste cotton to prepare a carbon-based adsorbent for the removal of lead ion and methylene blue from wastewater [26]. Sulfur-doped carbons were produced by carbonizing solid powder mixture in which SLS was used as a carbon precursor. The solid powders were carbonized at 500–900 °C for 2 h with a heating rate of 5 °C·min^{-1}. Prepared carbon materials were used for the photocatalytic degradation of tetracycline under visible-light irradiation [27]. CLS was pyrolyzed at 700 and 800 °C for 1 h with a heating rate of 5 °C/min. After washing carbonized materials with HCl and deionized water and drying, the prepared N-O-S co-doped hierarchical porous carbons were used in high-performance supercapacitor applications [28]. CLS, SLS, and alkali lignin were carbonized at 800 °C for 10 h without any additional templating/activation agent to prepare hierarchical porous carbons for the decolorization of wastewater dyes. It was reported that the prepared carbon materials (SLS-C, AL-C, and CLS-C with surface areas 346 m^2·g^{-1}, 405 m^2·g^{-1}, and 512 m^2·g^{-1}, respectively) showed excellent adsorption–decolorization abilities for five dyes [29]. The global annual production of apricots is substantial, and the seeds of this fruit can also be utilized by extracting seed oil. The apricot seed pulp resulting from this process is regarded as waste. Consequently, it is imperative to utilize this substantial amount of waste biomass. Furthermore, due to the presence of sulfonic groups in their structure, lignosulfonates were considered a suitable material for the production of biochar with promising and distinct properties through the co-pyrolysis with ASP. To the best of our knowledge, there is no study regarding the production of biochar from ASP and CLS/SLS. In this study, the pyrolysis of ASP, CLS, and SLS and the co-pyrolysis of ASP with CLS and SLS were carried out at temperatures ranging from 400 to 700 °C and ratios of 4:1, 1:1, and 1:4. The effect of raw material type, in addition to the effect of temperature, on the yields of biochars obtained as a result of co-pyrolysis was investigated. The synergistic effect of different types of materials on the elemental composition and HHVs of biochars obtained at different temperatures was investigated. The characteristics of biochars obtained from the pyrolysis process was also determined. The results obtained from this study are expected to contribute to the more effective utilization of waste/by-product from two different industries and to the production of sustainable carbon-based materials.

2. Materials and Methods

2.1. Procurement of Chemicals and Biomass Samples

ASP, SLS, and CLS were used as the biomass source in this study. ASP was obtained as a by-product of the mechanical pressing process carried out using the cold-press method at temperatures below 40 °C and was supplied by SNS Food and Cosmetics Trade and Industry Ltd. Co. (Tokat, Türkiye). Upon receipt, the ASP samples were dried under laboratory conditions for 24 h at room temperature. The dried material was sieved to obtain particle sizes in the range of 0.1–3 mm to standardize the particle size distribution. The resulting samples were stored in airtight containers until further analysis. SLS ($C_{20}H_{24}Na_2O_{10}S_2$, CAS No.: 8061-51-6) and CLS ($C_{20}H_{24}CaO_{10}S_2$, CAS No.: 8061-52-7) were of commercial purity and supplied by Obafer Chemical Industry and Trade Co., Ltd. (İzmir, Türkiye). The materials were stored under the supplier's recommended conditions and were used directly in the pyrolysis experiments without any further purification. Figure 1 shows ASP, SLS, and CLS.



Figure 1. Appearance of raw materials used in pyrolysis process: (**a**) ASP, (**b**) SLS, and (**c**) CLS.

Other chemicals used in the study, including anhydrous sodium sulfate (Na_2SO_4, CAS No.: 7757-82-6, ISOLAB GmbH, İstanbul, Türkiye) and hydrochloric acid (HCl, CAS No.: 7647-01-0, Fluka Chemie GmbH, Buchs, Switzerland), were of analytical grade and used as received.

2.2. Production of Biochars

The co-pyrolysis of ASP with CLS and SLS was carried out at 400–700 °C using a pyrolysis system consisting of a stainless-steel reactor heated by an electric furnace (Uniterm, Ankara, Türkiye) and a series of condensate collection vessels connected to the reactor outlet; a schematic diagram of this system is presented in Figure 2. This process resulted in the formation of biochar and bio-oil.

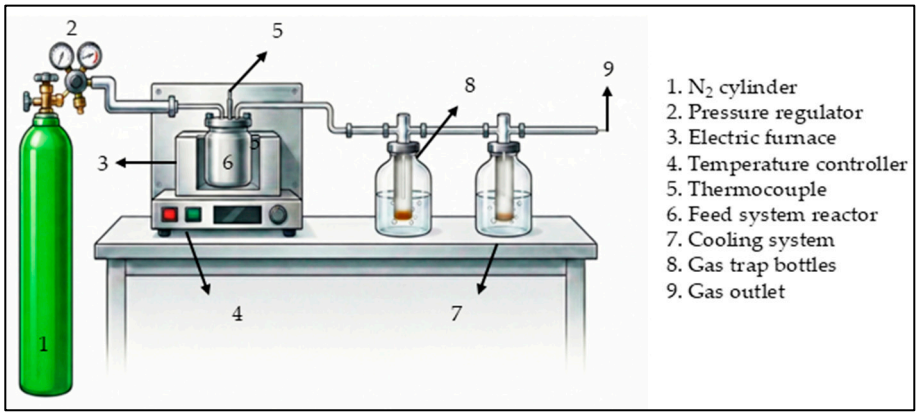


Figure 2. Schematic diagram of the pyrolysis system used for pyrolysis experiments.

Before being fed into the reactor, individual samples of ASP, CLS, and SLS, as well as mixtures of ASP with LSs (ASP-SLS and ASP-CLS), were prepared. The mixtures were formulated at three different ratios (4:1, 1:1, and 1:4), and a total of 10 g of sample was placed into the reactor for each experiment. After sealing, the reactor was purged with nitrogen gas (N_2) for 30 min to remove any residual air. Subsequently, the reactor was heated to the target temperature range (400–700 °C) at a constant heating rate of 10 °C·min^{-1} under a continuous flow of N_2 and maintained at that temperature for 1 h. Pyrolysis experiments were performed in triplicate, and the results were averaged.

During pyrolysis, the vapors produced were carried by the N_2 flow into the condensate collection vessels, where the bio-oil was condensed. After the heating period, the system was shut down and allowed to cool to room temperature under N_2 flow before opening. The biochars were removed from the reactor, weighed, and then immersed in 20 mL of 0.1 M HCl solution in order to remove inorganic salts and metal impurities. Subsequently, the samples were washed under vacuum with deionized water until the filtrate reached neutral pH. The washed biochars were dried at 103 ± 2 °C for 24 h and stored in sealed containers for characterization analyses. The biochar samples were designated as XASP–YLS–Z, where X:Y represents the mixing ratios of ASP and LS, and Z denotes the pyrolysis temperature. LS refers to either lignosulfonate (calcium or sodium).

2.3. Characterization of Raw Materials and Biochars

The proximate analysis parameters of the ASP biomass (moisture, volatile matter, ash, and fixed carbon) were determined in accordance with the ISO 18134-1:2015(E) [30], ISO 18123:2023(E) [31], and ISO 18122:2022(E) standards [32], and all analyses were performed in triplicate. The corresponding parameters for the CLS and SLS biomasses were used based on the analysis certificates provided by the supplier. Proximate analyses of ASP, SLS, and CLS are shown in Table 1.

Table 1. Proximate analyses of ASP, SLS, and CLS samples.

Raw Material	Moisture Content (%)		Volatile Matter (%)		Ash (%)		[a] Fixed Carbon (%)	
	Average	SD	Average	SD	Average	SD	Average	SD
ASP	3.66	0.26	88.88	0.04	2.84	0.07	4.61	0.23
SLS	5.36	0.20	56.58	0.39	17.70	-	20.36	0.59
CLS	6.44	0.09	55.00	0.62	16.85	-	21.71	0.72

[a] by difference.

The elemental composition of the biomass and biochar samples obtained from the pyrolysis experiments including carbon (C), hydrogen (H), nitrogen (N), and sulfur (S) was determined using an elemental analyzer (Elementar Vario MICRO Cube, Hessen, Germany). Functional group analyses were performed by Fourier Transform Infrared (FTIR) spectroscopy (Thermo Scientific Nicolet iS50 FTIR-ATR, Waltham, MA, USA) in the wavelength range of 4000–600 cm^{-1}. The surface morphology was examined using a field emission scanning electron microscope (FESEM, Carl Zeiss Ultra Plus Gemini, Baden-Württemberg, Germany). The crystalline structures were identified by X-ray powder diffraction (XRD) using a Rigaku Ultima IV diffractometer (Tokyo, Japan) with Cu Kα radiation (λ = 1.5406 Å) in the 2θ range of 10–90°, operating at 40 kV and 40 mA. The thermal behavior of the biomass was analyzed by thermogravimetric analysis (TGA) using a PerkinElmer STA 6000 instrument (Shelton, CT, USA) within the temperature range of 30–800 °C, at a heating rate of 10 °C·min^{-1}, under a nitrogen flow rate of 30 mL·min^{-1}. The weight-based yields of the biochars were calculated using Equation (1).

$$Biochar\ yield\ (wt\%) = \frac{Mass\ of\ recovered\ biochar\ (\mathrm{g})}{Intial\ mass\ of\ biomass\ (\mathrm{g})} \quad (1)$$

The higher heating values (HHV, MJ·kg^{-1}) of the biomass and biochar samples were calculated from their elemental composition using the Dulong equation (Equation (2); [33]):

$$HHV\left(\frac{\mathrm{MJ}}{\mathrm{kg}}\right) = \left[(0.338 \times C) + \left(1.428 \times \left(H - \frac{O}{8}\right) + (0.095 \times S)\right)\right] \quad (2)$$

3. Results and Discussion

3.1. Thermogravimetric Analysis of Raw Materials

Figure 3 shows TGA thermographs of ASP, CLS, and SLS. The first stage of thermal decomposition of the ASP was observed at 30–175 °C. This weight loss stage can be attributed to the removal of water and some volatile compounds in the structure of the ASP [34]. The weight loss which occurred at around 175–240 °C can be related to the volatilization of the hemicellulose content of the ASP biomass. The main decomposition of the cellulose and lignin content of the ASP can be attributed to the weight loss between 240 and 450 °C [34]. The ASP had the highest weight loss ratio among all samples. This may be due to the lower lignin content of the ASP when compared to LSs. The weight loss rate of the SLS was found to be

slightly higher than that of the CLS. A similar trend was reported in a previous study [35]. The weight loss stages of the CLS may include the removal of water in the structure (ca. 30–125 °C), intermolecular dehydration, formaldehyde removal, condensation reactions, the release of small molecules and the decomposition of the framework of the CLS (ca. 125–400 °C), the formation of calcium compounds and hydrocarbons via the reaction of small molecules with each other (400–550 °C and 550–750 °C) and the chemical decomposition of the previously mentioned compounds (above 750 °C) [36].

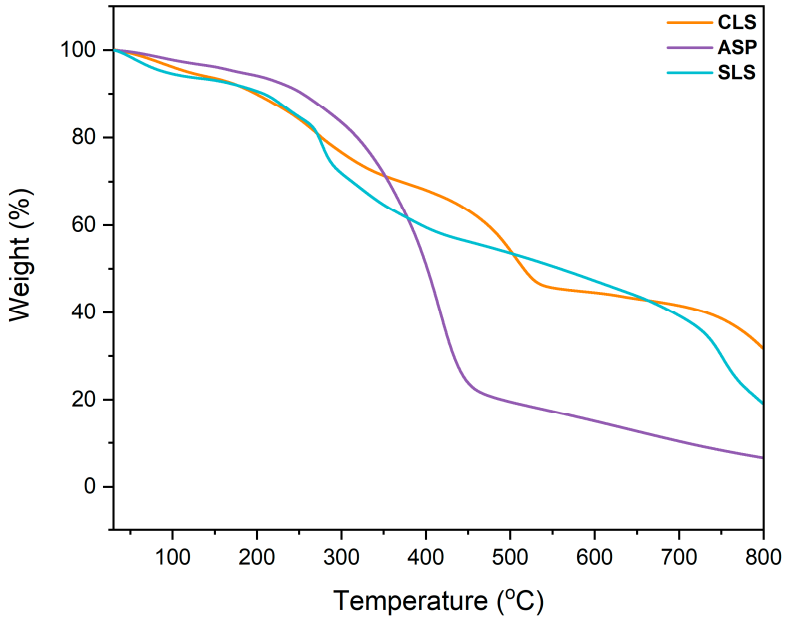


Figure 3. Thermal degradation characteristics of ASP, CLS, and SLS samples.

3.2. Biochar Yields

The biochar yields both calculated and obtained from the pyrolysis of the ASP and CLS alone, as well as their mixtures in different ratios (4:1; 1:1; 1:4) at different temperatures (400–700 °C), are presented in Figure 4. The biochar yields obtained from the individual pyrolysis of the ASP and CLS were found to be between 23.58 and 17.85 wt% and 52.97–48.25 wt%, respectively. Increasing the pyrolysis temperature from 400 to 700 °C resulted in a decrease in biochar yields for both feedstocks due to the further decomposition of raw materials and pyrolysis products. In case of ASP, increasing the temperature from 400 °C to 500 °C led to a noticeable decrease in biochar yields from 23.58 wt% to 19.62 wt%. A further increase in temperature resulted in a slight decrease in biochar yields. Biochar yields from the CLS slightly decreased with increasing the pyrolysis temperature up to 600 °C. A further increase in temperature resulted in a noticeable decrease in the CLS biochar yield. This can be attributed to the lignin content of the CLS. For similar reasons, biochar yields obtained from the CLS were found to be higher than those obtained from the ASP due to its higher lignin content. The biochar yields obtained from the co-pyrolysis of the ASP–CLS mixtures at different ratios and temperatures were between the char yields obtained from the pyrolysis of both raw materials individually. As the LS content in the mixtures increased, so the biochar yields also increased, approaching the levels observed in LS pyrolysis. At an elevated temperature of 500 °C, the biochar yields of the ASP–CLS mixtures, at ratios of 4:1, 1:1, and 1:4, were found to be 26.34, 34.95, and 45.15 wt%, respectively. Theoretical yields were found to be close to these values, at 26.20, 36.06, and 45.92 wt%, respectively.

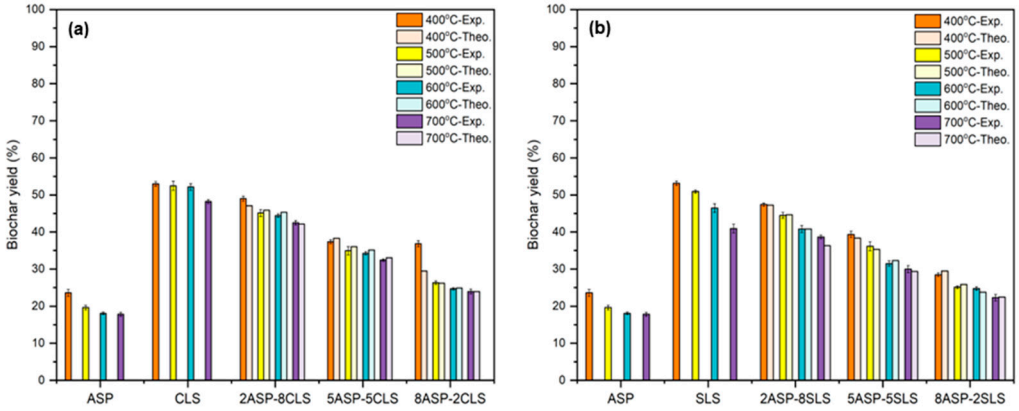


Figure 4. (**a**) Experimental and theoretical biochar yields obtained from pyrolysis of CLS, ASP, and their mixtures at 400–700 °C. (**b**) Experimental and theoretical biochar yields obtained from pyrolysis of SLS, ASP, and their mixtures at 400–700 °C.

A comparable trend has been observed in the comparison of actual and theoretical biochar yields at different pyrolysis temperatures. The properties and yields of biochars obtained from the pyrolysis of the SLS and cellulose mixtures at 500 °C were investigated in previous studies [37,38]. The actual biochar yields for all mixtures were found to be higher than the theoretical biochar yields [38]. It has been reported that the reason for obtaining higher actual biochar yields than theoretical biochar yields at 500 °C may be due to the inhibition of lignin pyrolysis by cellulose. In our study, the absence of such a trend can be attributed to the use of waste biomass with a more complex structure instead of cellulose. The difference between actual and theoretical yields may be attributed to the various factors related to the structural differences in raw materials, such as lignin, cellulose, hemicellulose, and ash content. The decomposition temperatures of biomass components, namely hemicellulose, cellulose, and lignin, are approximately in the ranges of 220 to 300 °C, 300 to 340 °C, and 300 to 900 °C, respectively [39]. It can be concluded that the differences between theoretical and actual yields may have arisen as a result of interactions between the products generated from those components during pyrolysis.

The biochar yields both calculated and obtained from the pyrolysis of the ASP and SLS alone, as well as their mixtures in different ratios (4:1; 1:1; 1:4) at different temperatures (400–700 °C), are presented in Figure 4. The biochar yields obtained from the individual pyrolysis of the ASP and SLS were found to be between 23.58 and 17.85 wt% and 53.17 and 40.92 wt%, respectively. Increasing the pyrolysis temperature from 400 °C to 700 °C resulted in a decrease in biochar yields for the SLS due to the further decomposition of raw materials and pyrolysis products. When comparing the biochar yields obtained from the pyrolysis of the SLS and CLS alone in Figure 4, the biochar yields obtained from the SLS at 600 and 700 °C (46.50 and 40.92 wt%) were noticeably lower than those obtained from the CLS (52.18 and 48.25 wt%). In another study, the pyrolysis characteristics of the CLS and SLS were investigated, and it was reported that the SLS exhibited greater weight loss than the CLS [40]. This could be due to the structural differences between the SLS and CLS. The presence of organically bonded sodium cations in the SLS can result in a major effect on the decomposition mechanism, thereby facilitating the dehydration and de-carboxylation reactions [41]. Biochar yields obtained from the SLS showed a decrease at a certain rate up to 600 °C, similar to those from the CLS; however, increasing the temperature to 700 °C resulted in a greater decrease in biochar yield.

The biochar yields obtained from the co-pyrolysis of the ASP–SLS mixtures at different ratios and temperatures were between the biochar yields obtained from the individual pyrolysis of raw materials. As the LS content in the mixtures increased, biochar yields

also increased, approaching the biochar yields from LS pyrolysis. In general, the actual and theoretical biochar yields of the mixtures at the same temperature were close to each other. At 500 °C, the actual biochar yields of the ASP–SLS mixture at ratios of 4:1, 1:1, and 1:4 were 25.10, 36.14, and 44.50 wt%, respectively; the theoretical yields were also close to these values, at 25.89, 35.29, and 44.69 wt%, respectively. A similar trend was also observed between actual biochar yields and theoretical biochar yields at pyrolysis temperatures of 600 and 700 °C. The ash content and composition of ash are important parameters in the pyrolysis process. They can affect the decomposition of biomass components and react with products formed during pyrolysis, which may result in differences in theoretical and actual biochar yields.

3.3. Bio-Oil Yields

The bio-oil yields, both calculated and experimentally obtained from the pyrolysis of the ASP, CLS, and SLS individually, as well as from their mixtures at different ratios (4:1; 1:1; 1:4) and at various temperatures (400–700 °C), are presented in Figure 5. The bio-oil yields obtained from the pyrolysis of the ASP alone showed a steady increase from 50.99% to 61.98% with rising temperature. Increasing the temperature from 400 °C to 700 °C promoted the thermal decomposition of the biomass structure, thereby increasing the bio-oil yield.

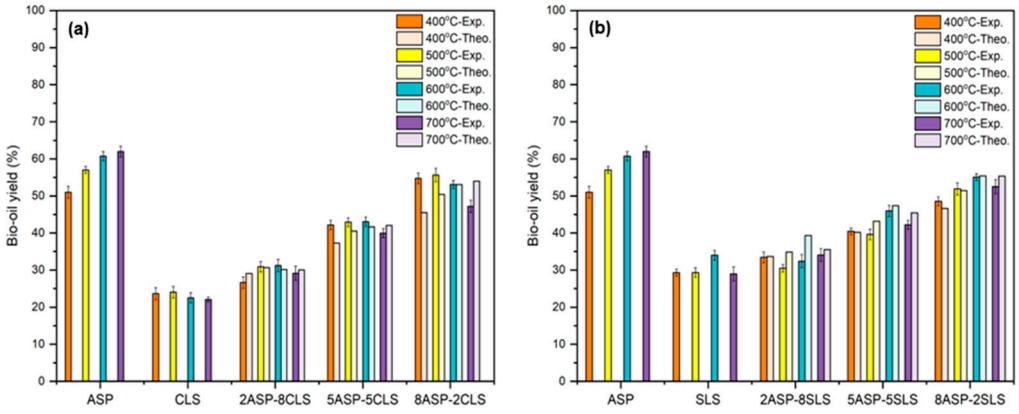


Figure 5. (**a**) Experimental and theoretical bio-oil yields obtained from pyrolysis of CLS, ASP, and their mixtures at 400–700 °C. (**b**) Experimental and theoretical bio-oil yields obtained from pyrolysis of SLS, ASP, and their mixtures at 400–700 °C.

In contrast, the bio-oil yields from the pyrolysis of the CLS and SLS alone were lower compared to the ASP. This demonstrates the tendency of high-lignin-content materials to yield lower amounts of liquid products during pyrolysis [42]. For the CLS, bio-oil yields were not affected by temperature and remained within a narrow range of 22.08% to 24.06%. For the SLS, the yields increased up to 600 °C, reaching 33.98%, but then decreased to 28.96% at 700 °C. Due to the high lignin content and aromatic structure of lignosulfonates, biochar formation is favored, resulting in lower liquid yields compared with the ASP. The slightly higher bio-oil yield of the SLS compared to the CLS may be attributed to the catalytic effect of sodium ions present in its structure.

When investigating the bio-oil yields obtained from the co-pyrolysis of the ASP–CLS mixtures, it was observed that increasing the proportion of ASP in the mixture also increased the bio-oil yield, approaching the yields obtained from the pure ASP pyrolysis. Notably, at 400 °C, the experimental bio-oil yield (54.75%) of the 8ASP–2CLS mixture was noticeably higher than the theoretically calculated value (45.52%). This can be due to the interaction of pyrolysis products during pyrolysis of the ASP and CLS at lower temperatures, promoting the formation of liquid products.

However, at 500 °C and 600 °C, for mixtures with a higher CLS content (5ASP–5CLS and 2ASP–8CLS), the experimental yields were generally close to the theoretical values, while at 700 °C the experimental yields were lower than predicted. This can be due to the interaction between formed products from the ASP and CLS, which results in a further decomposition during pyrolysis.

The bio-oil yields obtained from the co-pyrolysis of the ASP–SLS mixtures exhibited behavior different from the ASP–CLS mixtures. For the 8ASP–2SLS mixture, the experimental yield at 400 °C (48.55%) was slightly higher than the theoretical value (46.66%). However, as the temperature and SLS content increased, the experimental yields consistently fell below the theoretical predictions. This decrease was noticeable at all temperatures above 400 °C. For example, in the 2ASP–8SLS mixture at 600 °C, the theoretical yield was 39.33%, whereas the experimental yield was 32.38%. In conclusion, the co-pyrolysis of the ASP with lignosulfonates (especially CLS) created synergistic effects at specific ratios and temperatures, resulting in bio-oil yields exceeding theoretical expectations. However, the inorganic content and high LS proportions—particularly in the SLS compared to the CLS—exhibited a limiting effect on liquid product yields.

3.4. Elemental Composition of Biochars and Raw Materials

The elemental composition and HHV values of raw materials (ASP and CLS) and biochars obtained from the pyrolysis of the ASP-CLS mixtures are presented in Table 2. The HHV of the CLS was found to be 13.85 $MJ \cdot kg^{-1}$. The pyrolysis process led to deoxygenation as the oxygen content of all the biochars was found to be noticeably lower than that of both raw materials. The HHV of the CLS biochar (23.38 $MJ \cdot kg^{-1}$) was found to be noticeably higher than the HHV of the CLS. The HHVs of the biochars obtained from the pyrolysis of the CLS alone were found to be between 18.96 and 23.38 $MJ \cdot kg^{-1}$, which were noticeably higher than that of the raw material. The HHV of the biochar (27.14 $MJ \cdot kg^{-1}$) obtained from the pyrolysis of the ASP at 400 °C was found to be quite close to the HHV of the ASP raw material (27.81 $MJ \cdot kg^{-1}$). Increasing the pyrolysis temperature to 500 °C had a substantial impact on the calorific value of the ASP biochar, reducing it to 24.59 $MJ \cdot kg^{-1}$. A slight decrease in the HHVs of the ASP biochars was observed with further increases in temperature. The reason for obtaining biochars with lower HHVs can be attributed to the ash content of the biochars. Ash content remaining in the biochar post pyrolysis does not contribute to energy production, and this can result in a reduction in the HHVs of biochars [43].

When the same amount of the ASP was added to the CLS, the HHV of the biochar obtained at 400 °C (26.91 $MJ \cdot kg^{-1}$) was found to be very close to the HHV of the ASP-400 biochar (27.14 $MJ \cdot kg^{-1}$). This value is noticeably higher than the HHV of the biochar obtained from the pyrolysis of the CLS at 400 °C (23.38 $MJ \cdot kg^{-1}$). Furthermore, the HHVs of biochars obtained from all ASP-CLS mixture ratios in the pyrolysis process at 400 °C were found to be higher than the HHV of the biochar obtained from the pyrolysis of the CLS alone at 400 °C. A similar situation has been observed in biochars obtained from other pyrolysis temperatures. Among the biochars produced from the pyrolysis of the ASP-CLS mixtures, the biochar with the highest HHV (26.91 $MJ \cdot kg^{-1}$) was obtained from pyrolysis at 400 °C with a 1:1 ASP-CLS ratio; the HHV of the 8ASP-2CLS-400 biochar (26.11 $MJ \cdot kg^{-1}$) was quite close to this value. Based on these results, it can be concluded that using mixtures of the CLS and ASP instead of performing the pyrolysis of the CLS alone at a low pyrolysis temperature of 400 °C would be beneficial in obtaining biochars with a higher HHV.

The elemental composition and HHV values of the raw materials (ASP and SLS) and biochars obtained from pyrolysis of the ASP and SLS are presented in Table 3. The HHV of the SLS raw material was found to be 15.77 $MJ \cdot kg^{-1}$. The HHV of the SLS

biochar (22.11 MJ·kg^{-1}) obtained from pyrolysis at the lowest temperature was found to be noticeably higher than the SLS. At pyrolysis temperatures above 400 °C, the HHVs of the SLS biochars were higher than those of the CLS biochars. The highest HHV (25.64 MJ·kg^{-1}) in the ASP–SLS mixtures was obtained from the 8ASP to 2SLS-400 biochar. This value is higher than the HHV of the biochar (22.11 MJ·kg^{-1}) obtained from the pyrolysis of the SLS at the same temperature. The HHVs of biochars obtained at 400 °C were found to be noticeably affected by the ASP ratio in the mixture; as the ASP ratio in the mixture increased, the HHV of the biochar increased. However, this effect was observed to be diminished at higher pyrolysis temperatures. Based on these results, it can be concluded that using mixtures of the SLS and ASP instead of performing the pyrolysis of the SLS alone at a low pyrolysis temperature of 400 °C would be beneficial in obtaining biochars with a higher HHV.

Table 2. Elemental composition (%) and HHV (MJ·kg^{-1}) of biochars obtained from pyrolysis of CLS, ASP, and their mixtures.

Material	C%	H%	N%	S%	O% [a]	HHV [b] (MJ·kg^{-1})
ASP	58.59	8.97	5.33	0.13	26.98	27.81
CLS	41.02	5.41	0.82	6.13	46.62	13.85
ASP-400	69.16	4.82	8.07	0.32	17.63	27.14
CLS-400	62.91	4.3	8.66	1.04	23.09	23.38
2ASP-8CLS-400	66.17	4.04	8.79	0.43	20.57	24.50
5ASP-5CLS-400	68.73	4.87	7.54	0.33	18.53	26.91
8ASP-2CLS-400	68.54	4.42	7.72	0.31	19.01	26.11
ASP-500	68.75	3.43	7.90	0.02	19.90	24.59
CLS-500	58.36	3.06	7.27	1.67	29.64	18.96
2ASP-8CLS-500	60.19	2.96	6.79	1.14	28.92	19.52
5ASP-5CLS-500	63.32	3.08	7.1	0.52	25.98	21.21
8ASP-2CLS-500	66.93	3.28	7.48	0.20	22.11	23.38
ASP-600	71.28	2.45	7.23	0.04	19.00	24.20
CLS-600	61.09	2.8	4.10	1.92	30.09	19.46
2ASP-8CLS-600	62.67	3.01	5.00	2.54	26.78	20.94
5ASP-5CLS-600	65.06	2.37	5.55	1.94	25.08	21.08
8ASP-2CLS-600	68.08	2.32	6.42	0.82	22.36	22.41
ASP-700	71.46	2.24	6.05	0.06	20.19	23.75
CLS-700	62.39	3.17	3.17	2.79	28.48	20.80
2ASP-8CLS-700	62.77	3.03	3.48	1.74	28.98	20.54
5ASP-5CLS-700	65.30	2.78	5.07	1.67	25.18	21.71
8ASP-2CLS-700	69.62	2.04	5.22	0.43	22.69	22.44

[a] by difference, [b] calculated using Dulong formula.

Table 3. Elemental composition (%) and HHV (MJ·kg^{-1}) of biochars obtained from pyrolysis of SLS, ASP, and their mixtures.

Material	C%	H%	N%	S%	O% [a]	HHV [b] (MJ·kg^{-1})
ASP	58.59	8.97	5.33	0.13	26.98	27.81
SLS	48.53	4.11	2.73	5.37	39.26	15.77
ASP-400	69.16	4.82	8.07	0.32	17.63	27.14
SLS-400	64.44	3.45	1.17	3.40	27.54	22.11
2ASP-8SLS-400	66.28	3.55	2.05	2.79	25.33	23.22
5ASP-5SLS-400	68.21	3.89	3.74	1.91	22.25	24.82
8ASP-2SLS-400	69.21	3.99	5.93	0.99	19.88	25.64
ASP-500	68.75	3.43	7.90	0.02	19.90	24.59
SLS-500	66.70	3.32	1.24	2.96	25.78	22.97
2ASP-8SLS-500	66.14	3.07	1.74	2.96	26.09	22.36
5ASP-5SLS-500	66.74	3.07	3.15	2.40	24.64	22.77
8ASP-2SLS-500	67.19	3.05	5.22	1.48	23.06	23.09
ASP-600	71.28	2.45	7.23	0.04	19.00	24.20

Table 3. *Cont.*

Material	C%	H%	N%	S%	O% [a]	HHV [b] (MJ·kg^{-1})
SLS-600	74.14	2.51	1.26	3.90	18.19	25.77
2ASP-8SLS-600	69.70	2.25	1.94	2.98	23.13	22.93
5ASP-5SLS-600	71.34	2.33	3.42	2.38	20.53	24.00
8ASP-2SLS-600	71.34	2.47	4.96	1.27	19.96	24.20
ASP-700	71.46	2.24	6.05	0.06	20.19	23.75
SLS-700	71.39	2.23	1.18	4.62	20.58	24.08
2ASP-8SLS-700	71.30	1.86	1.78	3.64	21.42	23.28
5ASP-5SLS-700	73.46	1.91	3.32	2.91	18.40	24.55
8ASP-2SLS-700	73.20	2.00	4.71	0.89	19.20	24.25

[a] by difference, [b] calculated using Dulong formula.

Compared to similar studies in the literature, the HHVs of biochars were found to be higher than HHVs of biochars obtained from de-oiled seed cakes, including castor seed cake (21.8 MJ·kg^{-1}), flaxseed (22.3 MJ·kg^{-1}), and Calophyllum inophyllum (22.24 MJ·kg^{-1}) [44].

Similarly, the HHVs of the ASP–SLS biochars were also found to be higher than these values in most cases. However, the HHVs of most ASP-CLS biochars has been found to be relatively low compared to the biochars obtained from these cakes, with the exception of biochars produced at a low temperature.

3.5. FTIR Analysis of Biochars and Raw Materials

Functional groups on the surface of the biochars and raw materials were investigated by FTIR analysis (Figure 6). The peak observed at 3300–3310 cm^{-1} can be attributed to the stretching of hydroxyl groups, which indicates the presence of aromatics, alcohols, proteins, phenols, fiber, and water in the structure [45]. This peak cannot be observed in the structure of the biochars due to the effect of the pyrolysis process. The presence of hemicellulose, cellulose, and lignin in the structure can be demonstrated by the peak observed at around 2930–2910 cm^{-1}, which is attributed to aliphatic C-H stretching. The vibration of O-CH_3 in the lignin structure can be assigned to the peak observed at 2855 cm^{-1} [45]. The peak at 1740 cm^{-1} can demonstrate the presence of carbonyl groups, and the presence of C=C aromatic ring stretching and the N-H amine groups can be referred to the peak observed at 1650–1540 cm^{-1}. The increase in bands at 1600–1500 cm^{-1} with increasing temperature can be associated with the vibrations of aromatics [46]. The peak observed at 1462–1458 cm^{-1} can be attributed to the aromatic methyl group vibration which is due to the presence of cellulose and hemicellulose [45]. The presence of aryl group in the lignin can be referred to the peaks observed at 1235 cm^{-1}. The peaks which were related to the stretching of C-O can be observed at 1050–1060 cm^{-1} due to the presence of polysaccharides and lignin [45].

The aromatic skeleton vibration (C=C) of the lignin in LSs can be associated with the peaks observed at around 1598 cm^{-1}, 1511 cm^{-1}, and 1423 cm^{-1}. The peaks at around 1450 cm^{-1} can be attributed to the C-H bending vibrations of -CH_2- and -CH_3. The bands observed at around 1262 cm^{-1} and 1026 cm^{-1} can be attributed to the C-O and C-H groups of the guaiacyl unit of lignin [47]. S=O stretching, which represents -SO_3H groups in the SLS, can be associated with the band at around 1194 cm^{-1} and 1040 cm^{-1} [48]. The bands at 1040–1075 cm^{-1} in the CLS spectrum can be attributed to S=O stretching vibrations, which represent sulfonic acid groups [49]. As the CLS ratio in mixtures increases, an increase in the intensity of these bands in the biochar has been observed. Increasing the pyrolysis temperature from 600 to 700 °C resulted in a decrease in these bands. The decrease in bands, which is attributed to the stretching of SO_2 asymmetric (1420–1330 cm^{-1}) and SO_2 symmetric (1200–1145 cm^{-1}) groups, can be associated with the reduction in S=O groups during carbonization and their conversion to C-S (thiophene S) structures [50]. The band at around 650–600 cm^{-1} can be attributed the characteristics of the S-O band of LSs [47].

One of the possible applications of the biochar is soil remediation. The C and N functional groups on the biochar surface can form an organic mineral complex by interacting with multivalent iron oxide particles. The presence of functional groups such as OH, NH_2, and SH groups can reduce the mobility and bioavailablity of potentially toxic elements by adsorption and complexation with these elements [51]. The obtained biochar can be utilized for the removal of toxic heavy metals from wastewater in accordance with the functional groups it contains, including the amine, sulfone, and carbonyl groups [52].

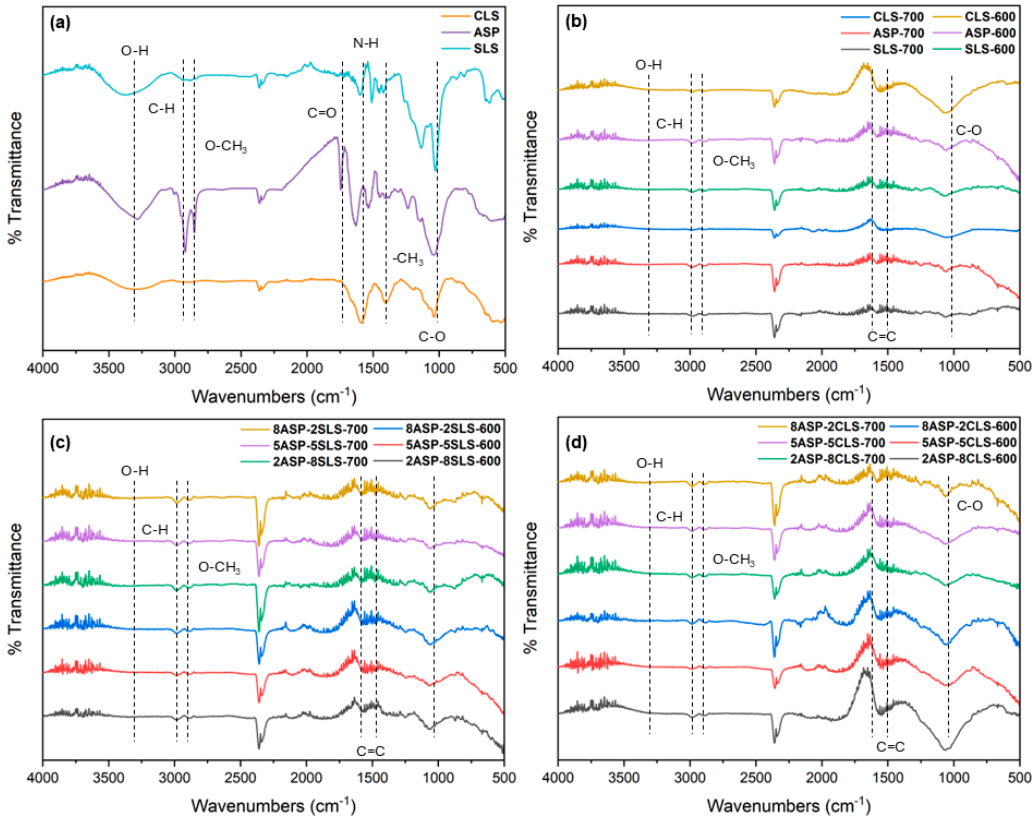


Figure 6. (**a**) FTIR spectra of CLS, ASP, and SLS samples, (**b**) FTIR spectra of CLS, ASP, and SLS biochars pyrolyzed at 600 °C and 700 °C, (**c**) FTIR spectra of ASP-SLS biochars prepared by mixing at different ratios and pyrolyzed at 600 °C and 700 °C, and (**d**) FTIR spectra of ASP-CLS biochars prepared by mixing at different ratios and pyrolyzed at 600 °C and 700 °C.

3.6. SEM Analysis of Biochars and Raw Materials

Figure 7 shows SEM images of the raw materials and biochars obtained from individual pyrolysis at different temperatures. It can be seen from the SEM images that the ASP and CLS have regularly shaped smooth surfaces in the structure, while the SLS has a less regularly shaped structure. The existence of small porous areas was also observed on the surface of the SLS. The formation of highly porous areas was observed on the surface of all biochars due to the pyrolysis process. The ASP and CLS biochars obtained at 600 and 700 °C have a more irregularly shaped structure and more porous areas on their surface when compared to the biochars obtained at lower pyrolysis temperatures. Increasing the temperature led to the formation of more porous areas on the surface of the SLS biochars. However, the existence of larger pores was observed on the surface of the SLS-700 biochar.

Figure 8 shows SEM images of the biochars obtained from the pyrolysis of the ASP, SLS, and CLS mixtures at 600 and 700 °C. The surface morphologies of all the biochars obtained from the pyrolysis of the ASP–SLS mixtures were similar at 600 °C. Increasing the pyrolysis temperature from 600 to 700 °C led to the formation of larger pores on the surfaces of the ASP-SLS biochars, which can be due to the further decomposition of the

carbonaceous structure. Porous areas were also observed on the surfaces of the biochar obtained from the pyrolysis of the mixtures of the ASP and CLS at 600 and 700 °C. It can be seen from the SEM images of the biochars at 700 °C that, as the CLS ratio in the mixture increased, more irregular structure and porous areas on the biochar's surface was observed. One of the desirable characteristics of a biochar for the removal of toxic metals from water and soil remediation is porosity. Therefore, increased porosity on the surface of a biochar makes it a good alternative for such applications [51,52].

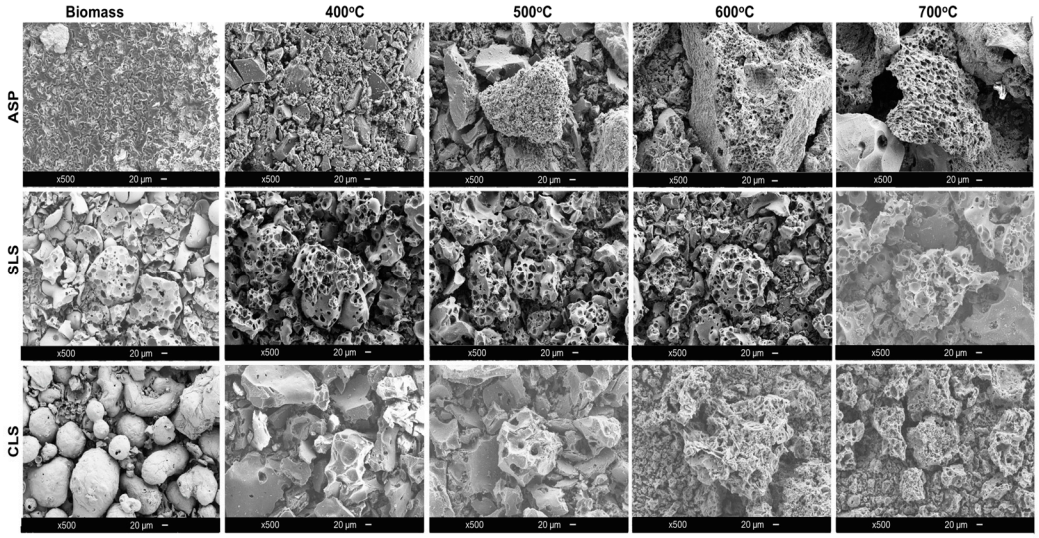


Figure 7. SEM images of CLS, ASP, and SLS and their corresponding biochars pyrolyzed at 400 °C, 500 °C, 600 °C, and 700 °C.

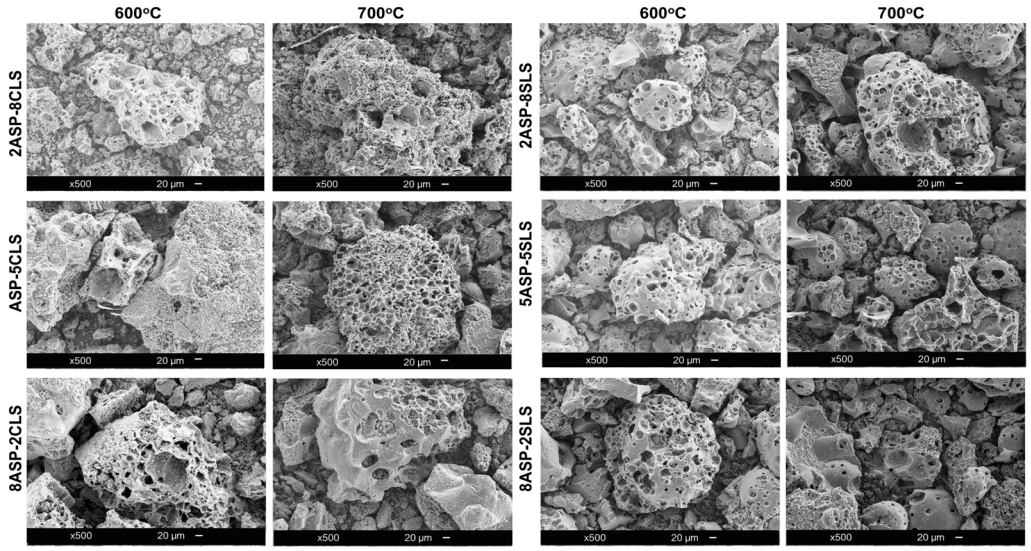


Figure 8. SEM images of ASP–CLS and ASP–SLS biochars prepared by mixing at different ratios and pyrolyzed at 600 °C and 700 °C.

3.7. XRD Analysis of Biochars and Raw Materials

The XRD patterns of the ASP, CLS, SLS and biochars obtained from pyrolysis are presented at Figure 9. The presence of crystalline and amorphous peaks in the XRD patterns of the biochars were observed. The diffraction peaks observed at 19.2°, 22.8°, 25.3°, 28.3°, 31.6°, 33.4°, 46.8°, 69.9°, and 71.8° in the XRD pattern of the biochar obtained from the pyrolysis of the SLS at 600 °C are consistent with the previous studies and show similarity to the characteristic pattern of the SLS [53,54]. The intensity of these peaks

has decreased noticeably for the biochar obtained at 700 °C, which can be related to an amorphous structure; this can be attributed to the greater decomposition of the biochar structure during pyrolysis at high temperature. The presence of inorganics (Na_2SO_4 and NaCl) in the SLS structure (JCPDS card: 00-001-0990 and 01-078-0751) can be demonstrated from the XRD pattern, which is consistent with a previous study [53]. The presence of $CaSO_4$ and $Ca(OH)_2$ crystalline phases in the structure is also considered (JCPDS card no: 00-003-0377 and 00-050-0008). The $CaSO_4$ phase is characterized by a peak observed around 25.6°, and peaks at 28.2°, 31.6°, 36.5°, and 38.8° also support the presence of this phase. The $Ca(OH)_2$ phase can be demonstrated by peaks at around 34.1° and 47.1°, and a small peak at approximately 18° also indicates the possible presence of this phase.

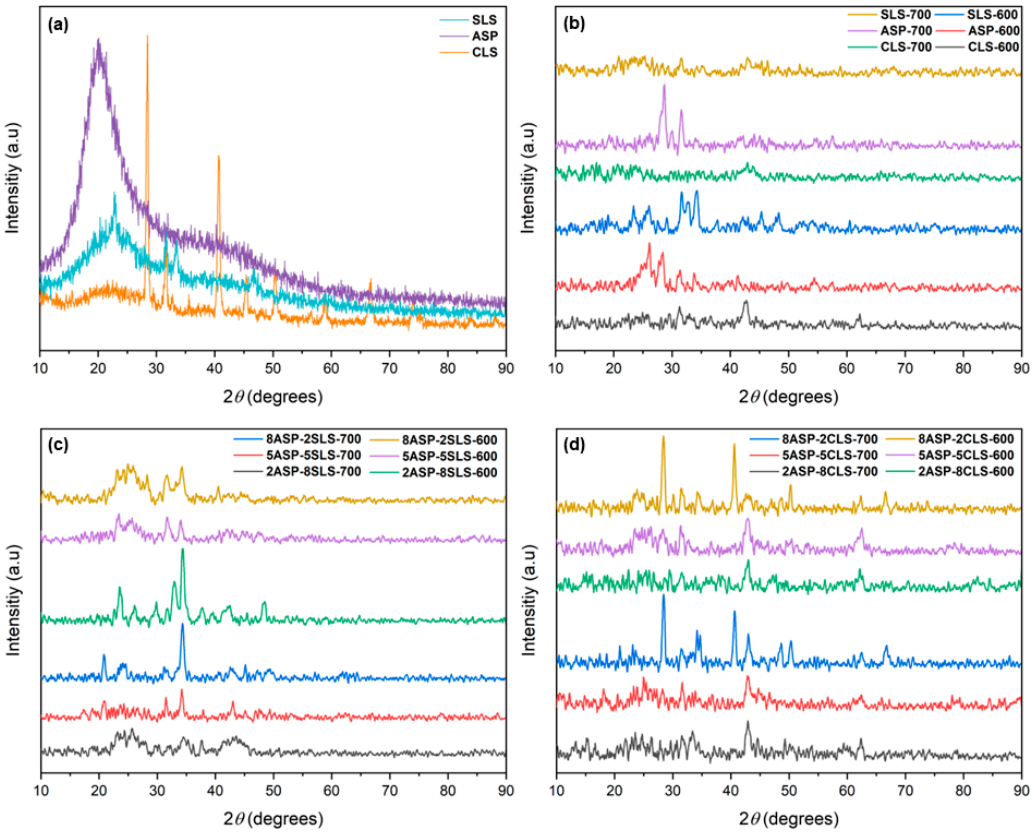


Figure 9. (**a**) XRD patterns of CLS, ASP, and SLS samples, (**b**) XRD patterns of CLS, ASP, and SLS biochars pyrolyzed at 600 °C and 700 °C, (**c**) XRD patterns of ASP–SLS biochars prepared by mixing at different ratios and pyrolyzed at 600 °C and 700 °C, and (**d**) XRD patterns of ASP–CLS biochars prepared by mixing at different ratios and pyrolyzed at 600 °C and 700 °C.

4. Conclusions

The co-pyrolysis of a waste from the essential oil industry and by-products from the paper pulp industry was performed in the study. For this purpose, ASP, CLS, and SLS were chosen as raw materials. The effect of temperature and biomass–LS ratio on the yields of biochar and the composition and characteristics of biochars were investigated. The produced biochars can be used as a biofuel due to their high HHVs. Biochars with higher HHVs were obtained with the addition of the ASP to the CLS. Consequently, the production of the ASP-CLS biochar instead of the CLS biochar will be more advantageous in terms of its use as a biofuel. The results showed that the ASP and LS ratios are important parameters for the characteristics of the biochars. The biochars produced have the potential for application in the treatment of wastewater and the remediation of soil, due to their porous structure and the presence of functional groups such as amine, sulfone, and carbonyl

on their surface. Bio-oil, another product of pyrolysis, has also been obtained with high yields. The elucidation of the properties of this bio-oil may allow for its use in applications such as energy production or as a chemical feedstock. The use of two different types of material has led to the production of biochars with different properties that have the potential to be used in various ways.

Author Contributions: Conceptualization, A.N.A., M.K.A., and H.Ş.K.; methodology, A.N.A., Y.B.H., and M.K.A.; writing—original draft preparation, A.N.A., Y.B.H., and M.K.A.; writing—review and editing, H.Ş.K., M.K.A., and A.N.A.; visualization, A.N.A. and Y.B.H. All authors have read and agreed to the published version of the manuscript.

Funding: This research was funded by Karabuk University Coordinatorship of Research Projects, grant number KBÜBAP-24-DS-142.

Data Availability Statement: The original contributions presented in this study are included in the article. Further enquiries can be directed to the corresponding author.

Acknowledgments: The authors utilized ChatGPT 5.2 Auto and a language model developed by OpenAI to enhance the text's spelling, punctuation, and style when preparing this piece. The writers take full responsibility for the publication's content after utilizing this tool/service, reviewing and editing it as necessary.

Conflicts of Interest: The authors declare no conflict of interest.

Abbreviations

The following abbreviations are used in this manuscript:

ASP	Apricot seed pulp
LS	Lignosulfonate
SLS	Sodium lignosulfonate
CLS	Calcium lignosulfonate
SEM	Field emission scanning electron microscope
TGA	Thermogravimetric analysis
FTIR	Fourier Transform Infrared spectroscopy
XRD	X-ray powder diffraction

References

1. Radenković, M.; Kovačević, M.; Radojičić, V.; Tošić, M.; Momčilović, M.; Živković, S. Corn Residue-Based Activated Carbon for Heavy Metal Removal: A Review of Adsorptive Performance and Properties. *Processes* **2025**, *13*, 3406. [CrossRef]
2. Rodriguez-Otero, A.; Vargas, V.; Galarneau, A.; Castillo, J.; Christensen, J.H.; Bouyssiere, B. Sustainable harnessing of SiO_2 nanoparticles from rice husks: A review of the best synthesis and applications. *Processes* **2023**, *11*, 3373. [CrossRef]
3. Devekıran, G.; Sarptaş, H. Torrefaction of Hazelnut Shells: The Effects of Temperature and Retention Time on Energy Yield and Fuel Characteristics. *Energies* **2025**, *18*, 4710. [CrossRef]
4. Razzak, S.A. Municipal solid and plastic waste derived high-performance biochar production: A comprehensive review. *J. Anal. Appl. Pyrolysis* **2024**, *181*, 106622. [CrossRef]
5. Ahmed, M.; Hameed, B. Insight into the co-pyrolysis of different blended feedstocks to biochar for the adsorption of organic and inorganic pollutants: A review. *J. Clean. Prod.* **2020**, *265*, 121762. [CrossRef]
6. Cai, W.; Wang, X.; Zhu, Z.; Kumar, R.; Amaniampong, P.N.; Zhao, J.; Hu, Z.-T. Synergetic effects in the co-pyrolysis of lignocellulosic biomass and plastic waste for renewable fuels and chemicals. *Fuel* **2023**, *353*, 129210. [CrossRef]
7. Sarıdaş, M.A.; Ağçam, E.; Ünal, N.; Akyıldız, A.; Kargı, S.P. Comprehensive quality analyses of important apricot varieties produced in Türkiye. *J. Food Compos. Anal.* **2024**, *125*, 105791. [CrossRef]
8. Makrygiannis, I.; Athanasiadis, V.; Chatzimitakos, T.; Mantiniotou, M.; Bozinou, E.; Lalas, S. Unveiling the Potential of Apricot Residues: From Nutraceuticals to Bioenergy. *Waste* **2024**, *2*, 1–28. [CrossRef]
9. Choi, D.; Kim, M.; Kim, J.Y.; Tsang, Y.F.; Jeong, S.; Kwon, E.E. Thermo-chemical processes for the sustainable utilization of oil-bearing biomass: A case study on apricot seed valorization. *Energy* **2024**, *302*, 131897. [CrossRef]

10. Li, S.; Xu, S.; Liu, S.; Yang, C.; Lu, Q. Fast pyrolysis of biomass in free-fall reactor for hydrogen-rich gas. *Fuel Process. Technol.* **2004**, *85*, 1201–1211. [CrossRef]
11. Petrova, B.; Budinova, T.; Tsyntsarski, B.; Kochkodan, V.; Shkavro, Z.; Petrov, N. Removal of aromatic hydrocarbons from water by activated carbon from apricot stones. *Chem. Eng. J.* **2010**, *165*, 258–264. [CrossRef]
12. Özbay, N.; Pütün, A. Characterization of chars from steam pyrolysis of apricot pulp. *Energy Sources Part A Recover. Util. Environ. Eff.* **2011**, *33*, 1504–1513. [CrossRef]
13. Manić, N.; Janković, B.; Pijović, M.; Waisi, H.; Dodevski, V.; Stojiljković, D.; Jovanović, V. Apricot kernel shells pyrolysis controlled by non-isothermal simultaneous thermal analysis (STA). *J. Therm. Anal. Calorim.* **2020**, *142*, 565–579. [CrossRef]
14. Yu, L.; Jia, R.; Liu, G.; Liu, X.; Hu, J.; Li, H.; Xu, B. Engineering a hierarchical reduced graphene oxide and lignosulfonate derived carbon framework supported tin dioxide nanocomposite for lithium-ion storage. *J. Colloid Interface Sci.* **2023**, *651*, 514–524. [CrossRef]
15. Zhou, M.; Sharma, B.K.; Li, J.; Zhao, J.; Xu, J.; Jiang, J. Catalytic valorization of lignin to liquid fuels over solid acid catalyst assisted by microwave heating. *Fuel* **2019**, *239*, 239–244. [CrossRef]
16. Zhao, H.-B.; Wang, W.-D.; Lü, Q.-F.; Lin, T.-T.; Lin, Q.; Yang, H. Preparation and application of porous nitrogen-doped graphene obtained by co-pyrolysis of lignosulfonate and graphene oxide. *Bioresour. Technol.* **2015**, *176*, 106–111. [CrossRef]
17. Wang, X.; Jiang, C.; Hou, B.; Wang, Y.; Hao, C.; Wu, J. Carbon composite lignin-based adsorbents for the adsorption of dyes. *Chemosphere* **2018**, *206*, 587–596. [CrossRef]
18. Wang, X.; Wang, J.; Jiang, L.; Jiang, Y. Adsorption of Pb^{2+} and Cu^{2+} in wastewater by lignosulfonate adsorbent prepared from corn straw. *Int. J. Biol. Macromol.* **2023**, *247*, 125820. [CrossRef]
19. Ma, Z.; Han, Y.; Wang, Q.; Wang, X.; Sun, G.; Li, Y. Construction of binary metal sulphides via lignosulfonate as sulphur source for efficient oxygen evolution reaction. *Int. J. Hydrogen Energy* **2023**, *48*, 9636–9646. [CrossRef]
20. Aro, T.; Fatehi, P. Production and application of lignosulfonates and sulfonated lignin. *ChemSusChem* **2017**, *10*, 1861–1877. [CrossRef]
21. Modrzejewska-Sikorska, A.; Robakowska, M.; Konował, E.; Gojzewski, H.; Gierz, Ł.; Wieczorek, B.; Warguła, Ł.; Łykowski, W. Lignin and Starch Derivatives with Selenium Nanoparticles for the Efficient Reduction of Dyes and as Polymer Fillers. *Coatings* **2023**, *13*, 1185. [CrossRef]
22. Dai, Q.; Liu, Q.; Yılmaz, M.; Zhang, X. Co-pyrolysis of sewage sludge and sodium lignosulfonate: Kinetic study and methylene blue adsorption properties of the biochar. *J. Anal. Appl. Pyrolysis* **2022**, *165*, 105586. [CrossRef]
23. Ma, J.; Khan, M.A.; Xia, M.; Fu, C.; Zhu, S.; Chu, Y.; Lei, W.; Wang, F. Effective adsorption of heavy metal ions by sodium lignosulfonate reformed montmorillonite. *Int. J. Biol. Macromol.* **2019**, *138*, 188–197. [CrossRef]
24. Cao, S.; Li, H.; Zhou, X.; Guo, H.; Chen, Y. NiS/activated carbon composite derived from sodium lignosulfonate for long cycle-life asymmetric supercapacitors. *J. Alloy. Compd.* **2022**, *900*, 163546. [CrossRef]
25. Dou, Z.; Zhang, Y.; Li, Z.; Fang, Z.; Li, H.; Fang, J. One-step preparation of lignin-based solid acid by carbonization and sulfonation to catalyze the synthesis of dimethyl adipate. *Ind. Crop. Prod.* **2022**, *180*, 114721. [CrossRef]
26. Fan, X.; Peng, L.; Wang, X.; Han, S.; Yang, L.; Wang, H.; Hao, C. Efficient capture of lead ion and methylene blue by functionalized biomass carbon-based adsorbent for wastewater treatment. *Ind. Crop. Prod.* **2022**, *183*, 114966. [CrossRef]
27. Liu, S.; Li, Q.; Zuo, S.; Xia, H. Facile synthesis of lignosulfonate-derived sulfur-doped carbon materials for photocatalytic degradation of tetracycline under visible-light irradiation. *Microporous Mesoporous Mater.* **2022**, *336*, 111876. [CrossRef]
28. Liu, Y.; Huang, G.; Li, Y.; Yao, Y.; Zhang, F.; Xing, B.; Zhang, C. N–O–S Co-doped hierarchical porous carbons derived from calcium lignosulfonate for high-performance supercapacitors. *Energy Fuels* **2020**, *34*, 3909–3922. [CrossRef]
29. Wu, Q.; Shao, W.; Zhang, Y.; Su, T.; Zhao, X.; Kong, F.; Xia, N.; Wang, Z. Use of lignin-based carbons for decolorization of wastewater dyes. *BioResources* **2020**, *15*, 105. [CrossRef]
30. *ISO 18134-1:2015*; Solid Biofuels-Determination of Moisture Content-Oven Dry Method, Part 1: Total Moisture, Reference Method. International Organization for Standardization: Geneva, Switzerland, 2015.
31. *ISO 18123:2023*; Solid Biofuels, Determination of Volatile Matter. International Organization for Standardization: Geneva, Switzerland, 2023.
32. *ISO 18122:2022*; Solid Biofuels, Determination of Ash Content. International Organization for Standardization: Geneva, Switzerland, 2022.
33. Tsarpali, M.; Kuhn, J.N.; Philippidis, G.P. Hydrothermal carbonization of residual algal biomass for production of hydrochar as a biobased metal adsorbent. *Sustainability* **2022**, *14*, 455. [CrossRef]
34. Fadhil, A.B. Evaluation of apricot (*Prunus armeniaca* L.) seed kernel as a potential feedstock for the production of liquid bio-fuels and activated carbons. *Energy Convers. Manag.* **2017**, *133*, 307–317. [CrossRef]
35. Huang, X.; Yin, H.; Zhang, H.; Mei, N.; Mu, L. Pyrolysis of Lignosulfonates and Lignin (De–Alkalization) via TG/DTG–FTIR/MS and In–Situ Py–PI–TOF/MS: Pyrolysis Characteristics, Gas Products, Volatiles, and Thermo–Kinetics. *SSRN Preprint* **2022**, 35. [CrossRef]

36. Chen, X.Y.; Zhou, Q.Q. The production of porous carbon from calcium lignosulfonate without activation process and the capacitive performance. *Electrochim. Acta* **2012**, *71*, 92–99. [CrossRef]
37. Zhao, C.; Ge, L.; Wang, R.; Chu, H.; Mai, L.; Zha, W.; Wang, Y.; Xu, C. Effects of cellulose addition on the physicochemical properties, pore structure and iodine adsorption of lignin-based biochar. *Fuel* **2023**, *352*, 129061. [CrossRef]
38. Ge, L.; Zhao, C.; Wang, Y.; Qi, Z.; Wang, R.; Yin, Q.; Zhang, Y.; Xu, C. Effects of cellulose addition on sodium lignosulfonate pyrolysis: Product distribution and formation pathway. *Can. J. Chem. Eng.* **2025**, *103*, 1285–1294. [CrossRef]
39. El-Sayed, S.A.; Khass, T.M.; Mostafa, M.E. Thermal degradation behaviour and chemical kinetic characteristics of biomass pyrolysis using TG/DTG/DTA techniques. *Biomass Convers. Biorefinery* **2024**, *14*, 17779–17803. [CrossRef]
40. Huang, X.; Yin, H.; Zhang, H.; Mei, N.; Mu, L. Pyrolysis characteristics, gas products, volatiles, and thermo–kinetics of industrial lignin via TG/DTG–FTIR/MS and in–situ Py–PI–TOF/MS. *Energy* **2022**, *259*, 125062. [CrossRef]
41. Jakab, E.; Faix, O.; Till, F.; Székely, T. Thermogravimetry/mass spectrometry of various lignosulfonates as well as of a kraft and acetosolv lignin. *Holzforschung* **1991**, *45*, 355–360. [CrossRef]
42. Mohan, D.; Pittman, C.U., Jr.; Steele, P.H. Pyrolysis of wood/biomass for bio-oil: A critical review. *Energy Fuels* **2006**, *20*, 848–889. [CrossRef]
43. Kandpal, S.; Tagade, A.; Sawarkar, A.N. Critical insights into ensemble learning with decision trees for the prediction of biochar yield and higher heating value from pyrolysis of biomass. *Bioresour. Technol.* **2024**, *411*, 131321. [CrossRef]
44. Rajpoot, L.; Tagade, A.; Deshpande, G.; Verma, K.; Geed, S.R.; Patle, D.S.; Sawarkar, A.N. An overview of pyrolysis of de-oiled cakes for the production of biochar, bio-oil, and pyro-gas: Current status, challenges, and future perspective. *Bioresour. Technol. Rep.* **2022**, *19*, 101205. [CrossRef]
45. Sahoo, A.; Kumar, S.; Mohanty, K. A comprehensive characterization of non-edible lignocellulosic biomass to elucidate their biofuel production potential. *Biomass Convers. Biorefinery* **2022**, *12*, 5087–5103. [CrossRef]
46. Naydenova, I.; Radoykova, T.; Petrova, T.; Sandov, O.; Valchev, I. Utilization perspectives of lignin biochar from industrial biomass residue. *Molecules* **2023**, *28*, 4842. [CrossRef] [PubMed]
47. Wibowo, E.S.; Park, B.-D. Chemical and thermal characteristics of ion-exchanged lignosulfonate. *Molecules* **2023**, *28*, 2755. [CrossRef] [PubMed]
48. Karpukhina, E.A.; Volkov, D.S.; Proskurnin, M.A. Quantification of lignosulfonates and humic components in mixtures by ATR FTIR spectroscopy. *Agronomy* **2023**, *13*, 1141. [CrossRef]
49. Rwei, S.-P.; Lien, C.-C. Synthesis and viscoelastic characterization of sulfonated chitosan solutions. *Colloid Polym. Sci.* **2014**, *292*, 785–795. [CrossRef]
50. Huang, R.; Tang, Y.; Luo, L. Thermochemistry of sulfur during pyrolysis and hydrothermal carbonization of sewage sludges. *Waste Manag.* **2021**, *121*, 276–285. [CrossRef]
51. Wu, Y.; Yan, Y.; Wang, Z.; Tan, Z.; Zhou, T. Biochar application for the remediation of soil contaminated with potentially toxic elements: Current situation and challenges. *J. Environ. Manag.* **2024**, *351*, 119775. [CrossRef]
52. Aziz, K.H.H. Removal of toxic heavy metals from aquatic systems using low-cost and sustainable biochar: A review. *Desalination Water Treat.* **2024**, *320*, 100757. [CrossRef]
53. Pang, J.; Zhang, W.; Zhang, H.; Zhang, J.; Zhang, H.; Cao, G.; Han, M.; Yang, Y. Sustainable nitrogen-containing hierarchical porous carbon spheres derived from sodium lignosulfonate for high-performance supercapacitors. *Carbon* **2018**, *132*, 280–293. [CrossRef]
54. Ji, X.; Guo, M.; Zhu, L.; Du, W.; Wang, H. Synthesis mechanism of an environment-friendly sodium lignosulfonate/chitosan medium-density fiberboard adhesive and response of bonding performance to synthesis mechanism. *Materials* **2020**, *13*, 5697. [CrossRef]

Disclaimer/Publisher's Note: The statements, opinions and data contained in all publications are solely those of the individual author(s) and contributor(s) and not of MDPI and/or the editor(s). MDPI and/or the editor(s) disclaim responsibility for any injury to people or property resulting from any ideas, methods, instructions or products referred to in the content.